Spatially Modulated Metamaterial Array for Transmit (SMMArT) and Slow-Leaky-Wave Antennas

Alessandro Salandrino, Patrick M. McCormick, Mario D. Balcazar, and Shannon D. Blunt
Radar Systems Lab (RSL), University of Kansas
Lawrence, KS, USA

***Abstract*—Waveform diversity (WD) has the potential to profoundly impact radar operation through new advantageous uses of design degrees-of-freedom as long as the waveform and signal processing structure can be appropriately married to the physical electromagnetic (EM) and system operation. Within this context, the EM behavior of the recently introduced Spatially Modulated Metamaterial Array for Transmit (SMMArT) concept, itself a realization of a special class of MIMO radar denoted as spatial modulation, is analyzed by means of full-wave finite-elements simulations. Radiation patterns under various forms of excitation are calculated. A parametric study of a slotted Clarricoats-Waldron waveguide (CWW) is presented that identifies the practical feasibility of design constraints that must be considered in order to suppress undesired intermodal coupling.**

Keywords—Slow Waves; Slotted Waveguides; Leaky Wave Antennas; Metamaterials; MIMO Radar; Spatial Modulation.

I. Introduction

To achieve many of the promised advances of waveform diversity (WD) [1-3] in practical radar systems necessitates a holistic perspective in which all aspects of the radar operation are considered, from the physical electromagnetic interface to the waveforms and signal processing [4,5]. The particular WD topic of multiple-input multiple-output (MIMO) radar has received significant attention over the last decade [6], along with controversy over realism and practical application to existing modalities [7,8]. The physical realization of MIMO radar requires consideration of the fundamental constraints imposed by the underlying physics of electromagnetic radiation in addition to the signal processing attributes and waveform characteristics. Therefore, merging electromagnetic theory, signal processing, and radio frequency (RF) system engineering is necessary.

Fast-time spatial modulation represents a special-case of MIMO that mimics the actuation of the human eye by generating a coherent transmit beam that moves about a center look direction during each pulse [9,10], thereby coupling the space and range dimensions which increases the degrees the freedom available for receive processing [11]. Being based on FM waveforms that maintain a coherent beam, spatial modulation is less susceptible than general MIMO to mutual coupling effects [12-14] and avoids the problem of "emitting" into the invisible space [15,16]. In fact, spatial modulation actually subsumes the frequency diverse array (FDA) concept [17-20] by permitting arbitrary beam-steering in fast-time.

Recently, a particular implementation of this emission scheme, denoted as the Spatially Modulated Metamaterial Array for Transmit (SMMArT) [21], was conceived by inspiration from slow-light optics [22,23]. The SMMArT implementation enables fast-time spatial modulation without requiring the hardware complexity of separate arbitrary waveform generation capability at every antenna element/subarray. In its simplest instantiation the SMMArT structure comprises a serially-fed slotted waveguide possessing a metamaterial dielectric core (to provide slow group velocity) and driven by a single waveform generator, yet it can realize spatial modulation in one dimension and readily emulate the FDA [17-20] when driven by a linear FM (LFM) waveform [21]. It is envisioned that more sophisticated versions will provide 2D spatial modulation [16] as well as fast-time polarization modulation [24]. Here a computational electromagnetic study of SMMArT is presented along with evaluation of the far-field emission generated when the SMMArT structure is driven by an arbitrary FM waveform.

II. SMMArT Principle of Operation

The SMMArT architecture is a generalization of the well-known slotted waveguide frequency scanned array (e.g. [25-27]) to incorporate FM pulse compression, a concept that was first proposed by Milne in 1964 [28]. The specific attributes of SMMArT are 1) use of a metamaterial dielectric core to achieve slow group velocity and 2) leveraging the structure of new FM waveform implementation/optimization methods (e.g. [29-33]). Collectively, these factors establish a design space that encompasses both the electromagnetic operation of the slotted waveguide array and the waveform structure to facilitate their joint optimization for the far-field emission.

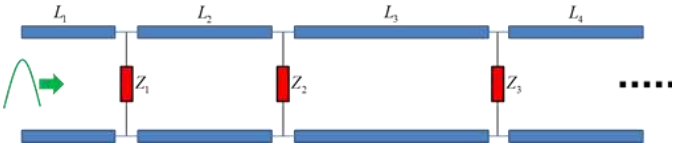

Figure 1. Schematic of a serially-fed array of antennas represented by their imput impedances Z_i.

SMMArT is based on a constrained series traveling-wave (non-resonant) feed architecture, as schematically illustrated in Figure 1. In terms of beam-steering mechanism, SMMArT departs from conventional frequency-scanned leaky-wave antennas [34] by virtue of relying on a slow-group-velocity

transmission line in order to perform intra-pulse and inter-pulse radiation-pattern modulation.

Per Figure 1, consider an idealized model in which the shunt impedences distributed along the transmission-line are the radiation resistances of a set of identical isotropic radiators located at the Cartesian positions $\boldsymbol{r}_n=(0,0,z_n)$. The current density over the radiating elements can be written as

$$J(z,t)=\sum_n I_n(t)\delta(z-z_n)\,. \tag{1}$$

We assume a voltage waveform at the generator with amplitude $V_0(t)$ and phase $\varphi(t)$ such that

$$V(t)=V_0(t)e^{-j\varphi(t)}\,. \tag{2}$$

The amplitudes $I_n(t)$ are related to the input voltage waveform of (2) as

$$I_n(t)=\frac{1}{Z_n}V_0\left(t-\frac{z_n}{v_g}\right)e^{-j\varphi\left(t-\frac{z_n}{v_p}\right)} \tag{3}$$

where v_g and v_p are the group velocity and phase velocity, respectively.

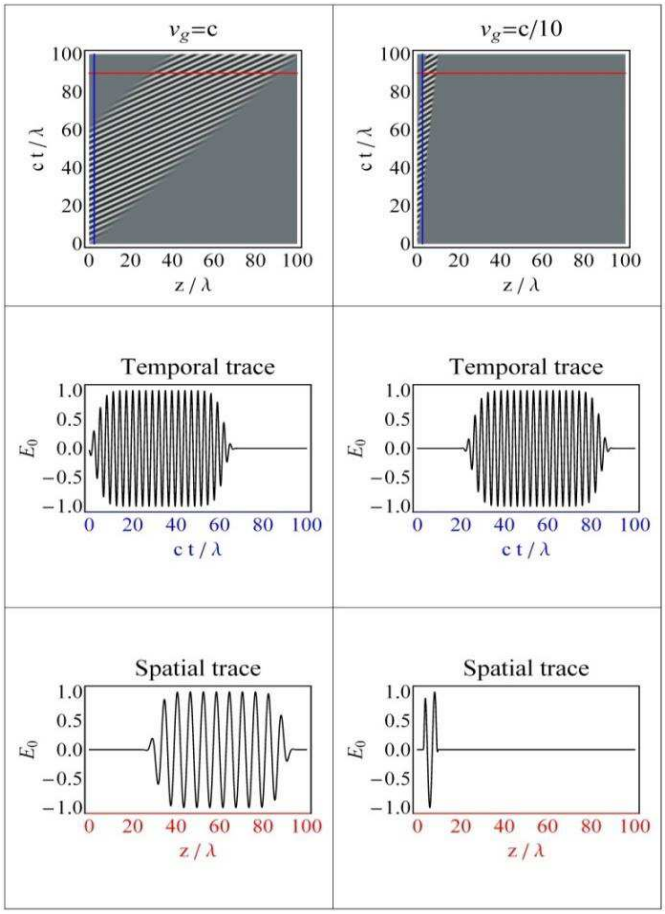

Figure 2. Spatial and temporal distribution of a pulse in a waveguide with group velocity $v_g=c$ (left column) and in a waveguide with $v_g=c/10$ (right column). All distances are normalized with respect to the vacuum wavelength λ. The temporal traces are evaluated over the blue lines, and the spatial traces are evaluated over the red lines.

The radiated far-field in spherical coordinates can be obtained from Jefimenko's equations [35] applied to (1) and (3) as

$$E(r,\theta,t)=\frac{1}{r}\sum_{n=1}^{N}\frac{1}{Z_n}V_0\left[\left(t-\frac{r}{c}\right)-\frac{z_n}{v_g}\right]e^{j\phi\left[t-\frac{r}{c}\left(1-\frac{z_n\cos\theta}{r}\right)-\frac{z_n}{v_p}\right]}\,. \tag{4}$$

In general, (4) can be applied to any serially-fed array, where the distinctive feature of the SMMArT array is a low-group-velocity transmission line, i.e. $v_g << c$.

The low-group-velocity transmission line employed in SMMArT serves the purpose of compressing the *spatial* extent of the waveform along the transmission line feeding the radiating elements. Neglecting group velocity dispersion effects, the spatial extent of a pulse of duration τ propagating in a transmission line is approximately $d = v_g \tau$. In a transmission line operating in the fundamental TEM mode in air where $v_g \approx c$, a pulse having a temporal duration of τ = 100 μs would have a spatial extent of d = 30 km, thereby far exceeding the dimensions of any practical array. As a result, essentially the same portion of the waveform would encounter all radiating elements simultaneously and the beam would be static, with the direction determined by the feed system delays alone.

However, a low group-velocity ($v_g << c$) feed-line would make the pulse much shorter in space. This concept is illustrated in Figure 2 which compares the spatial and temporal extent of a pulse propagating in a transmission line with high and low group-velocity. As apparent from the spatial traces (bottom row), the waveform spatial extent is significantly compressed in the latter. In a low group-velocity waveguide different portions of the waveform encounter the radiating elements at a given time, thereby allowing for far-field emission design to be accomplished through joint design of the waveform and the serial feed system.

Figure 3a illustrates a far-field emission generated by a 20 element slotted SMMArT having the dispersion relation discussed in the next section (Figure 8) and excited with an upchirped LFM waveform of 100 MHz bandwidth centered at 10 GHz and pulse duration 1 μs. In this case the fast-time spatial modulation realizes a linear beamsteering during the pulse such as could be accomplished using FDA [17-20]. The corresponding delay/angle ambiguity function [36] for the same configuration is shown in Figure 3b.

Figure 4 shows the time-domain and frequency domain radiation pattern of a SMMArT (with dispersion relation of Figure 8) having 30 radiating elements with inter-element separation of 15mm. This array is excited with a random polyphase-coded frequency-modulated (PCFM) waveform [29,30] centered at 10 GHz with 200 MHz bandwidth, pulse duration of 1 μs, and power spectrum shown in Figure 5. Note that the main lobe of the spectral radiation pattern shown in Figure 4b mirrors exactly the group velocity distribution of the SMMArT feed line. Figure 6 illustrates the delay/angle ambiguity function for this emission. Such a mode may have utility in tracking applications by mimicking the fixational movement of the human eye [9,10] to modify the delay/angle ambiguity function in an adaptive/cognitive manner.

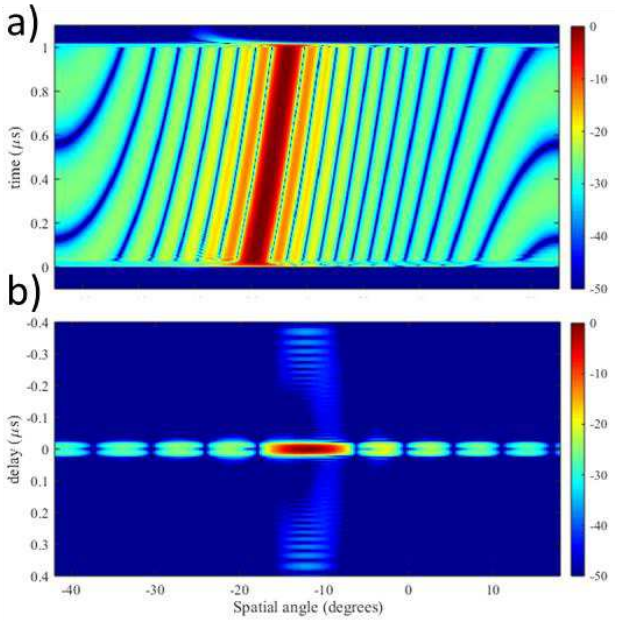

Figure 3. a) Far-field of a 20 element SMMArT that is fed with an upchirped LFM waveform with 100MHz bandwidth centered at 10GHz and pulse duration 1µs and b) the corresponding delay-angle ambiguity function [36].

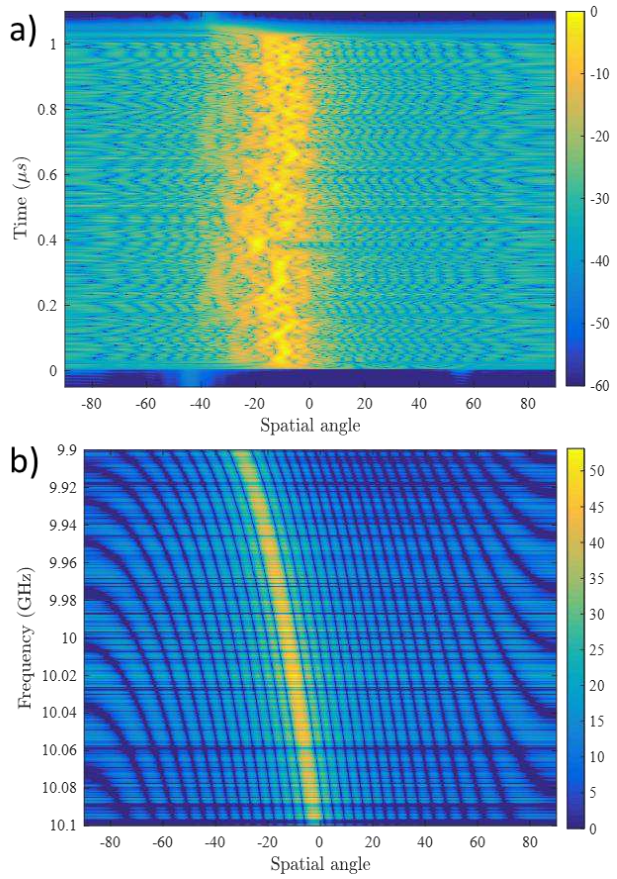

Figure 4. a) Time-domain and b) frequency domain radiation pattern of a 30 elements SMMArT, excited with a random polyphase-coded frequency-modulated (PCFM) waveform centered at 10 GHz with 200 MHz bandwidth and pulse duration of 1 µs.

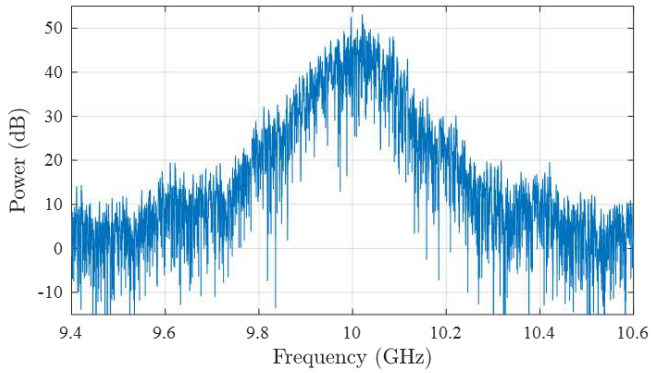

Figure 5. Power spectrum of random PCFM waveform

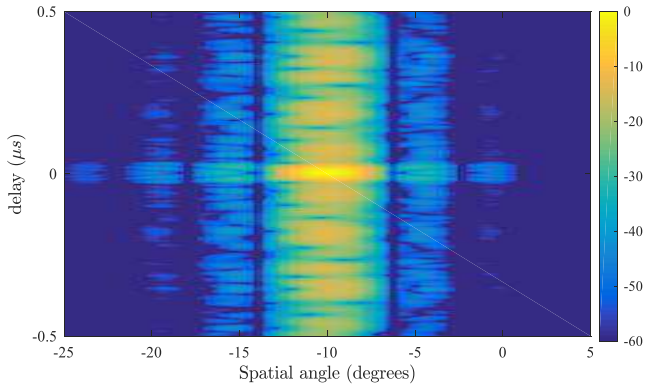

Figure 6. Delay-angle ambiguity function for SMMArT driven by a random polyphase-coded FM waveform

The radiation patterns displayed in Figure 3 and 4 are calculated under ideal single-mode operation of the slow-wave transmission line. In practice such conditions are difficult to achieve because of intermodal coupling in the proposed slow-wave transmission line. In Sections III and IV a physical realization of such a transmission line is presented, along with a discussion of the measures to be taken in order to approach ideal single-mode operation.

III. Slow Group Velocity Clarricoats-Waldron Waveguide

In this section we describe a physical realization of the low group velocity feed line that serves as the foundation of SMMArT. This system relies on a slotted waveguide of the Clarricoats-Waldron type [22,23]. The Clarricoats-Waldron waveguide (CWW) features two essential elements: (i) a hollow metallic waveguide that is (ii) coaxially loaded with a high permittivity rod. An example layout for X-band operation is shown in Figure 7.

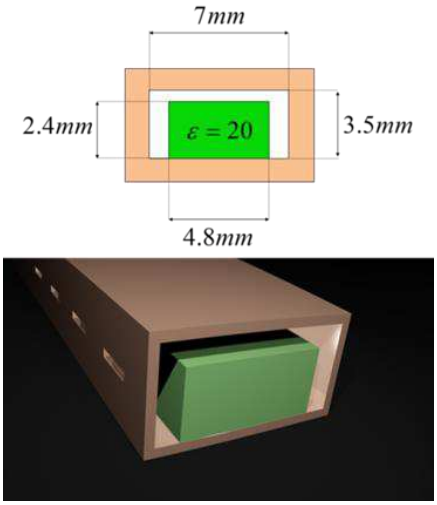

Figure 7. Layout of a slotted rectangular Clarricoats-Waldron waveguide for operation around 10GHz.

This inhomogeneous waveguide system is unique in that it supports backward modes (i.e. with antiparallel phase and group velocity), in spite of the fact that the structure is uniform in the propagation direction. The dispersion relation associated with the structure of Figure 7, which is designed to operate around 10GHz, is shown in Figure 8. The negative slope branch of the dispersion curve (shown in red) is indicative of a backward-wave mode. The blue branch on the other hand indicates a forward-wave mode. Notice that for frequencies in the 10GHz – 11GHz interval, two degenerate forward-wave and backward-wave modes are allowed. Interestingly, around 10GHz, where the two branches coalesce, the dispersion curve flattens out, indicating a vanishing group velocity.

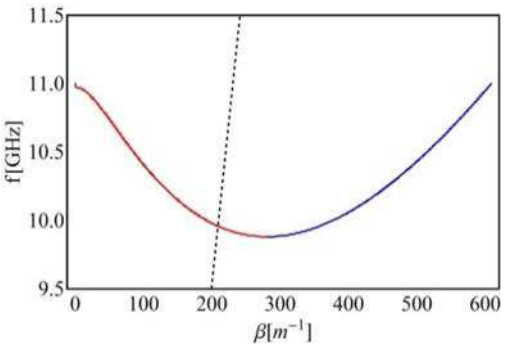

Figure 8. Dispersion relation for a Clarricoats-Waldron waveguide. The red branch and the blue branch indicate the backward-wave and forward-wave modes, respectively. In the frequency range from 10GHz to 11GHz the two modes coexist, while for frequencies above 11GHz only the forward-wave mode is supported. The dashed black line indicates the light-line.

The electric and magnetic field distributions of the fundamental backward mode at 10 GHz are shown in Figure 9. The reversal of the magnetic lines of force around the two convective regions visible in Figure cause the Poynting vector to change sign and become negative for positions external to the green line shown in Figure 9, where the Poynting vector vanishes. This power flow reversal results in the low-group velocity regime observed in the dispersion curve of Figure 8.

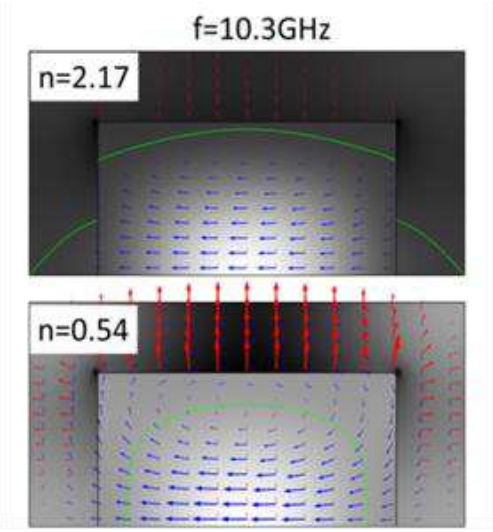

Figure 9. Modal field distribution and effective indices of the forward-wave mode (top) and of the backward-wave mode (bottom). The red and blue arrows indicate the electric and the magnetic fields, respectively. The green line denotes the region of zero Poynting vector.

IV. Electromagnetic Properties of a Slotted Clarricoats-Waldron Waveguide

To use a CWW for the physical realization of SMMArT, a mechanism must be introduced to allow the appropriate guided mode to radiate energy into free space. As in conventional slotted waveguide arrays (SWA), slits opened on either the broad wall or the narrow wall of the metallic enclosure of the CWW will allow radiation to leak out of the waveguide mode, with a radiation pattern determined, to first order perturbation, by the modal phase at the slit locations.

One essential difference exists between a CWW and a conventional waveguide, which facilitates new interesting possibilities to control the radiation patterns, but also makes the design or radiating slits more challenging in the case of CWW. This characteristic is the coexistence, at the same frequency, of two different field configurations associated with the same mode, as can be seen from the dispersion relation shown in Figure 8. We will improperly refer to these field configurations of the fundamental mode as “modes”.

Assuming that the CWW is excited with the fast backward-wave mode (red branch of the dispersion curve), a set of radiating slits with sub-wavelength separation would tend to radiate, depending on the frequency of operation, in the angular sector from broadside towards backfire. This interesting and useful feature cannot occur in a simple straight section of SWA without introducing grating lobes, or without the use of complex delay lines. One difficulty arises because the fast backward-wave mode and the slow forward-wave mode (blue branch of the dispersion curve) are not orthogonal in terms of polarization or field distribution. For this reason any structural perturbation of the waveguide can, and in fact will, lead to a power exchange between the two modes, which prevents the antenna from radiating under the desired single backward mode regime.

We have conducted a parametric study using a commercial finite element solver to determine a slit configuration that suppresses, or at least mitigates, the undesired coupling between forward and backward CWW modes. We have only considered horizontal slits on the narrow metallic wall of the waveguide. The two main geometrical parameters that affect intermodal coupling are slit length and axial position. To gauge the effect of slit length we simulated a CWW with a single slit of varying length.

Two representative electric field distributions are shown in Figure 10 for a CWW operating at 10GHz and excited with the backward mode. The mode is launched into the waveguide at the port indicated by the red arrow. Figure 10a shows the optimum configuration with a slit of length 5mm. In this case, less than 10% of the incident power is transferred from the backward mode to the forward mode. It is evident that the instantaneous electric field distribution along the waveguide maintains its spatial periodicity before and after the slit, indicating negligible reflection and mode conversion. The opposite situation is shown in Figure 10b for a slit length of 9mm, where a nearly complete power transfer to the forward mode is observed, as is clear from the different periodicity of the instantaneous electric field distribution.

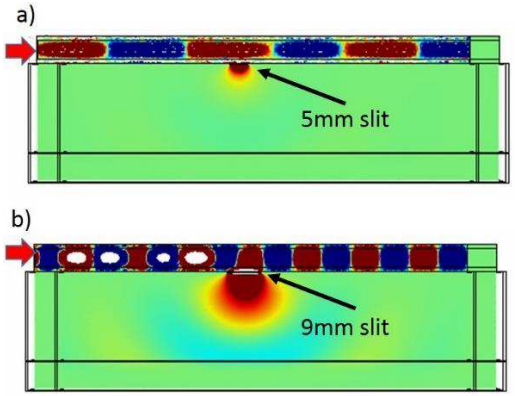

Figure 10. Electric field distribution in CWW Waveguide with a) a 5mm and b) 9mm slit on the narrow wall.

The other parameter that plays a fundamental role in this power transfer effect between backward and forward modes is the slit separation, which should be tuned so as to induce a destructive interference among the forward wave contributions generated at each slit. Figure 11 shows the near-field and radiation pattern at 10GHz of an array of ten 5mm-wide slits having an optimum separation between slits of 17mm. The directive beam observed in the far-field is consistent with the backward radiation expected from the backward CWW mode, i.e. the red-branch of the dispersion of Figure 8.

For comparison, in Figure 12 the near-field distribution and far-field radiation pattern are shown for a slit separation of 15mm. The coupling with the forward mode in this case produces the broadside lobe evident in the radiation pattern. The parametric analysis presented here shows that the issues related to the presence of two simultaneous modes can be addressed by careful design of the radiating elements to provide destructive interference for the unwanted mode.

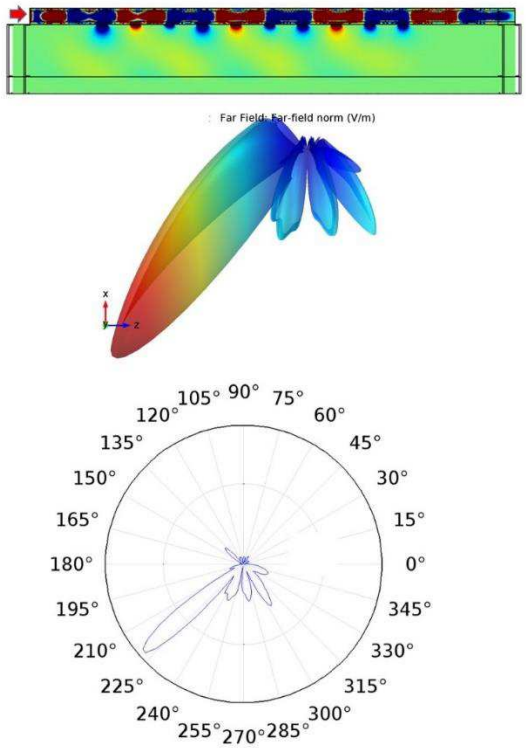

Figure 11. Near-field and radiation pattern of a slotted CWW with ten 5mm slits on the narrow wall separated by 17mm.

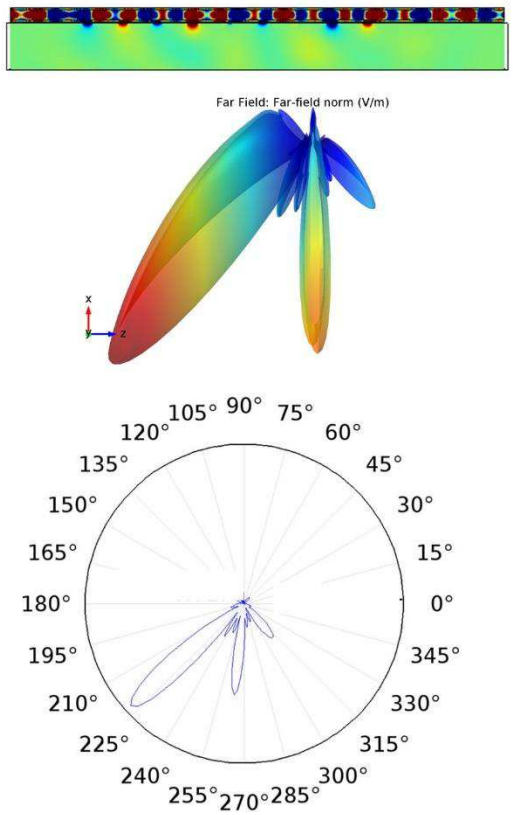

Figure 12. Near-field and radiation pattern of a slotted CWW with ten 5mm slits on the narrow wall separated by 15mm.

V. Conclusions

The recently proposed SMMArT structure, a form of Clarricoats-Waldron waveguide, provides a holistic framework within which to consider the antenna electromagnetics and the waveform in a joint manner. Here a parametric study of the electromagnetic properties of SMMArT was presented. It has been shown that the challenges arising because of the coexistence of two modes can be effectively addressed by careful design of the radiating slits. Combined with parametric structures for FM waveforms, this overall concept is a step towards facilitating the design of far-field emissions through joint transmitter/waveform optimization.

VI. References

[1] M. Wicks and E. Mokole, *Principles of waveform diversity and design*: The Institution of Engineering and Technology, 2011.

[2] U. Pillai, K. Y. Li, I. Selesnick, and B. Himed, *Waveform diversity*: McGraw-Hill, 2011.

[3] F. Gini, *Waveform design and diversity for advanced radar systems*: The Institution of Engineering and Technology, 2012.

[4] H. Griffiths, S. Blunt, L. Cohen, and L. Savy, "Challenge problems in spectrum engineering and waveform diversity," in *2013 IEEE Radar Conference (RadarCon13)*, 2013, pp. 1-5.

[5] S. D. Blunt and E. L. Mokole, "An overview of radar waveform diversity," *to appear in IEEE Aerospace & Electronic System Magazine*.

[6] J. Li and P. Stoica, *MIMO radar signal processing*: Wiley Online Library, 2009.

[7] E. Brookner, "MIMO radar demystified and where it makes sense to use," in *2014 International Radar Conference*, 2014, pp. 1-6.

[8] F. Daum and J. Huang, "MIMO radar: Snake oil or good idea?," in *2009 International Waveform Diversity and Design Conference*, 2009, pp. 113-117.

[9] S. D. Blunt, P. Mccormick, T. Higgins, and M. Rangaswamy, "Physical emission of spatially-modulated radar," *IET Radar, Sonar & Navigation,* vol. 8, pp. 1234-1246, 2014.

[10] P. McCormick and S. D. Blunt, "Fast-time 2-D spatial modulation of physical radar emissions," in *Radar Symposium (IRS), 2015 16th International*, 2015, pp. 505-510.

[11] P. M. McCormick, T. Higgins, S. D. Blunt, and M. Rangaswamy, "Adaptive receive processing of spatially modulated physical radar emissions," *IEEE Journal of Selected Topics in Signal Processing,* vol. 9, pp. 1415-1426, 2015.

[12] B. Cordill, J. Metcalf, S. A. Seguin, D. Chatterjee, and S. D. Blunt, "The impact of mutual coupling on MIMO radar emissions," in *Electromagnetics in Advanced Applications (ICEAA), 2011 International Conference on*, 2011, pp. 644-647.

[13] G. Babur, P. J. Aubry, and F. Le Chevalier, "Antenna coupling effects for space-time radar waveforms: analysis and calibration," *IEEE Transactions on Antennas and Propagation,* vol. 62, pp. 2572-2586, 2014.

[14] L. Savy and M. Lesturgie, "Coupling effects in MIMO phased array," in *2016 IEEE Radar Conference (RadarConf)*, 2016, pp. 1-6.

[15] G. J. Frazer, Y. I. Abramovich, and B. A. Johnson, "Spatially waveform diverse radar: Perspectives for high frequency OTHR," in *2007 IEEE Radar Conference*, 2007, pp. 385-390.

[16] P. M. McCormick, S. D. Blunt, and J. G. Metcalf, "Joint spectrum/beampattern design of wideband FM MIMO radar emissions," in *2016 IEEE Radar Conference (RadarConf)*, 2016, pp. 1-6.

[17] P. Antonik, M. C. Wicks, H. D. Griffiths, and C. J. Baker, "Frequency diverse array radars," in *2006 IEEE Conference on Radar*, 2006, p. 3 pp.

[18] T. Higgins and S. D. Blunt, "Analysis of range-angle coupled beamforming with frequency-diverse chirps," in *2009 International Waveform Diversity and Design Conference*, 2009, pp. 140-144.

[19] P. F. Sammartino, C. J. Baker, and H. D. Griffiths, "Frequency diverse MIMO techniques for radar," *IEEE Transactions on Aerospace and Electronic Systems,* vol. 49, pp. 201-222, 2013.

[20] W.-Q. Wang, "Overview of frequency diverse array in radar and navigation applications," *IET Radar, Sonar & Navigation,* vol. 10, pp. 1001-1012, 2016.

[21] A. Salandrino, D. J. C. Farfan, P. McCormick, E. D. Symm, and S. D. Blunt, "Spatially Modulated Metamaterial Array for Transmit (SMMArT)."

[22] P. Clarricoats and R. Waldron, "Non-periodic Slow-wave and Backward-wave Structures†," *International Journal of Electronics,* vol. 8, pp. 455-458, 1960.

[23] A. Salandrino and D. N. Christodoulides, "Negative index Clarricoats-Waldron waveguides for terahertz and far infrared applications," *Opt Express,* vol. 18, pp. 3626-31, Feb 15 2010.

[24] P. McCormick, J. Jakabosky, S. D. Blunt, C. Allen, and B. Himed, "Joint polarization/waveform design and adaptive receive processing," in *2015 IEEE Radar Conference (RadarCon)*, 2015, pp. 1382-1387.

[25] Y. J. Cheng, W. Hong, and K. Wu, "Millimeter-wave half mode substrate integrated waveguide frequency scanning antenna with quadri-polarization," *IEEE Transactions on Antennas and Propagation,* vol. 58, pp. 1848-1855, 2010.

[26] J. H. Choi, J. S. Sun, and T. Itoh, "Frequency-scanning phased-array feed network based on composite right/left-handed transmission lines," *IEEE Transactions on Microwave Theory and Techniques,* vol. 61, pp. 3148-3157, 2013.

[27] G. Gentile, V. Jovanović, M. J. Pelk, L. Jiang, R. Dekker, P. de Graaf, *et al.*, "Silicon-filled rectangular waveguides and frequency scanning antennas for mm-wave integrated systems," *IEEE Transactions on Antennas and Propagation,* vol. 61, pp. 5893-5901, 2013.

[28] K. Milne, "The combination of pulse compression with frequency scanning for three-dimensional radars," *Radio and Electronic Engineer,* vol. 28, p. 89, 1964.

[29] S. D. Blunt, M. Cook, J. Jakabosky, J. De Graaf, and E. Perrins, "Polyphase-coded FM (PCFM) radar waveforms, part I: implementation," *IEEE Transactions on Aerospace and Electronic Systems,* vol. 50, pp. 2218-2229, 2014.

[30] S. D. Blunt, J. Jakabosky, M. Cook, J. Stiles, S. Seguin, and E. Mokole, "Polyphase-coded FM (PCFM) radar waveforms, part II: optimization," *IEEE Transactions on Aerospace and Electronic Systems,* vol. 50, pp. 2230-2241, 2014.

[31] J. M. Kurdzo, B. L. Cheong, R. D. Palmer, and G. Zhang, "Optimized NLFM pulse compression waveforms for high-sensitivity radar observations," in *2014 International Radar Conference*, 2014, pp. 1-6.

[32] J. Jakabosky, S. D. Blunt, and B. Himed, "Waveform design and receive processing for nonrecurrent nonlinear FMCW radar," in *2015 IEEE Radar Conference (RadarCon)*, 2015, pp. 1376-1381.

[33] J. Jakabosky, S. D. Blunt, and B. Himed, "Spectral-shaped optimized FM noise radar for pulse agility," in *IEEE Radar Conf*, 2016.

[34] A. A. Oliner and D. R. Jackson, "Leaky-wave antennas," *Antenna Engineering Handbook,* vol. 4, p. 12, 1993.

[35] O. D. Jefimenko, *Electricity and magnetism*: Appleton-Century-Crofts, 1966.